ULE™ - Zero Expansion, Low Density, and Dimensionally Stable Material for Lightweight Optical Systems

Suresh T. Gulati and Mary J. Edwards
Corning Incorporated
Corning, NY 14831

ABSTRACT

The zero expansion titania-silica binary glass ULE™ offers an optimum combination of thermal, mechanical, and optical properties which make it an ideal material for precision optical structures and lightweight telescope mirrors. Its near-zero thermal expansion over the ambient operating temperature range helps preserve optical figure; the absence of hysteresis in its thermal expansion curve ensures dimensional stability of the mirror in extreme environments; its low density affords high specific stiffness thereby reducing elastic deformation of lightweight structures; its high fatigue resistance permits higher long-term stress without compromising mechanical reliability; and its excellent optical and birefringence properties facilitate inspection and quality assurance in terms of thermal expansion homogeneity, defect level, and residual strain.

This paper reviews the key physical properties of ULE glass and the various fabrication techniques available for making lightweight mirrors. Special emphasis is given to ULE's mechanical behavior which controls the long-term reliability of mirror blanks during fabrication, shipping, installation, and operation. It describes the 8-meter class mirror blank manufacturing process and the stress/time histories to which such blanks are exposed. These parameters, together with strength and fatigue data, were used to optimize surface finish for adequate strength and to evaluate an 8-meter blank support system to ensure long-term reliability of the blank during transportation. The paper concludes with recent advances and development programs in support of the manufacture of precision optical mirror blanks.

Keywords: ULE™, mirror blank, strength, fatigue, reliability, sagging, acid etching.

1. INTRODUCTION

ULE, a binary titania-silica glass made by Corning,* offers dimensional stability due to its essentially zero thermal expansion coefficient over a wide temperature range representative of operating ambient conditions. This glass is manufactured by the flame hydrolysis process which introduces chemical vapors into gas-oxygen burners at

*ULE™ is a trademark of Corning Incorporated. ULE is available as Corning Code 7971. Corning is currently in the process of developing an alternate process using different raw materials to produce ULE, which will be marketed as Corning Code 7972

approximately 1700°C. The combustion reaction forms sub-micron size molten titania-silica particles. The burners are aligned over a rotating table where the particles are collected and fused into a large dense solid boule of ULE, typically 1.5 m in diameter by 15 cm thick. Homogeneity is ensured through strict process control and by utilizing high-purity chemicals that are not subject to the ordinary compositional variations and contaminants of sand and other raw materials of conventional glass melting processes. The coefficient of thermal expansion (CTE) of ULE is dependent on the glass composition and is therefore subject to tight process control and minimal process variation. ULE is an amorphous, binary glass with no crystalline phases present. This differentiates it from other low expansion materials, such as the glass-ceramics Zerodur®† and AstroSitall‡ whose properties are dependent on controlled crystal growth in a glassy matrix. ULE is isotropic, meaning that its properties are the same in all directions, at any given location in a mirror or structure. This is critical for the predictability and preservation of optical figure.

2. MIRROR MATERIAL REQUIREMENTS

The material and techniques for fabricating mirrors are major considerations for the success of any telescope. Modern mirrors consist of a reflecting surface made up of a single or multiple layer dielectric film and a substrate. Only the thin reflecting layer applied on the first surface serves an optical purpose, while the substrate is the mechanical means to hold the reflecting surface in the proper contour during operation.

Two of the fundamental material requirements, according to Rodkevich and Robachevskaya,[1] for large precision mirrors are:

1. The mirror material must have appropriate physical properties which ensure high immunity to outside influences (low mechanical and temperature distortions), spatial isotropy, and dimensional stability over time;

2. The mirror material must be capable of accepting a high-quality polished surface and be coatable with materials having the required reflection coefficient.

To achieve precision optical performance, the substrate material should have minimum thermal expansion over the operating temperature range, exhibit dimensional stability over time and in extreme environments, and have high thermal diffusivity to minimize distortion associated with transient temperature gradients. In addition, high specific stiffness to minimize self-weight deflection and low mass are also desirable properties for the mirror material. The long-term mechanical integrity of the mirror material must be sufficient for the expected lifetime of the optical system, including i) surviving the rigors of manufacturing, handling, transportation, launch, and gravity release requirements in the case of satellite systems, ii) operation at different elevation angles for large terrestrial telescopes, and iii) centrifugal accelerations of high speed scanning and chopping optics and other structures such as microlithography stages.[2] The key properties of ULE and other near-zero expansion mirror materials are summarized in Table 1.

A more indepth discussion of several of the most important properties of ULE glass appears in the next section.

†Zerodur® is a registered trademark of Schott Glass Technologies.
‡AstroSitall is designated as C0115M.

Table 1. Key Properties of Mirror Materials

MATERIAL	Corning ULE	Zerodur®	AstroSitall
Mean CTE, ppb/K at room temp	0 ± 30	0 ± 50	0 ± 50
Temporal stability, ppm/yr	-0.025	-0.100	--
Thermal hysteresis	not detected	present	present
Thermal conductivity, w/m-K	1.31	1.46	1.19
Mean specific heat, J/kg-K	766	821	710
Thermal diffusivity, 10^{-4} m^2/s	0.008	0.007	0.006
Density, $10^3 kg/m^3$	2.20	2.53	2.46
Elastic modulus, GPa	67	92	92
Specific stiffness, 10^6 m	3.1	3.7	3.7
Poisson's ratio	0.17	0.24	0.24
Knoop hardness, kg/mm^2	460	620	--
Strength, psi, 220-240 grit finish	7740	8610	8460
Fracture toughness, $MPa\sqrt{m}$	0.70	0.85	0.80

3. KEY PHYSICAL PROPERTIES OF ULE

THERMAL PROPERTIES

The specification for the linear coefficient of thermal expansion of ULE is $0 \pm 30 \times 10^{-9}$/°C (ppb/°C) over the 5°C to 35°C temperature interval. This is the only true zero expansion material available with such a tight specification on CTE uniformity. Zero thermal expansion is key to maintaining mirror figure with temperature changes. For such a low expansion material, the spatial variations in CTE from point to point are often comparable to the maximum absolute value of CTE at any point. In this case, the changes caused by a completely uniform change in temperature level must be evaluated.[3]

All ULE boules are fully characterized for CTE using the nondestructive method described below. Since the actual CTE within any mirror blank is known in advance of fabrication, finite element modeling can be used to predict the performance of the planned mirror due to temperature changes. In the case of Corning's 8-m diameter mirror blanks, which are made by fusing over 80 individual boules of ULE together, finite element analysis is performed prior to fusing the boules. This predicts the mirror figure change that will occur after moving the polished mirrors to their telescope enclosures, located atop high mountains, where the temperature change from that of the polishing facility is significant. Such finite element modeling and analyses allow engineers, before actual mirror blank fabrication begins, to confirm their selection of appropriate CTE matching boules and to assure a quality mirror that will meet the error budget specified by optical designers.[3,4] A representative example of this analysis is given in Figure 1. A unique feature of ULE is that a rapid, nondestructive determination and documentation of thermal expansion coefficient of the actual mirror blank material is possible. Commonly, with other materials, an estimate of expansivity is obtained by testing samples of material believed similar to the final product, since test specimens cannot be obtained from the product without violating its integrity. With ULE, which is approximately 92.5% SiO_2 and 7.5% TiO_2, nondestructive testing of expansivity is possible

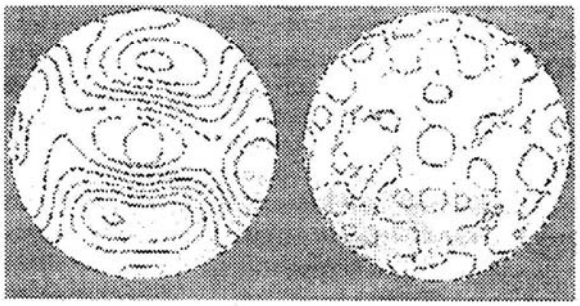

Figure 1. Finite Element Model for Analyzing Changes in Mirror Figure due to an Isothermal Temperature Change

because both ultrasonic velocity and expansivity correlate linearly with titania content. A simple measurement of ultrasonic transit time through the ULE glass and accurate measurement of its thickness lead to the CTE value with an uncertainty of less than 2 ppb/°C.[5,6] This unique characteristic permits selection and control of any CTE variation within a product, and has been successfully utilized by the Corning ULE manufacturing facility for process control and product certification since 1973. When a difference in CTE exists between any two pieces of ULE, it is constant, independent of temperature, permitting differential measurements to be made at room temperature that will apply to all temperatures between -200°C and 900°C. Measurement of the actual component parts assures that the final product will meet the demanding requirements of CTE homogeneity while exhibiting near-zero CTE. In the case of three 8-m diameter mirror blanks, independent verification of the differential boule CTE measurements was carried out photoelastically by measuring the small residual strains at the fusion seals between hexagons in the final blanks.[7] Figure 2 illustrates the excellent correlation between the two methods. The data follow a Gaussian distribution, and the small differences between the two methods are due to random error in the measurement techniques.

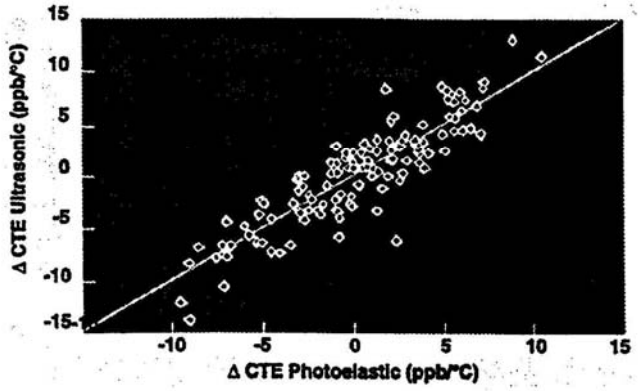

Figure 2. Comparison of ΔCTE at Fusion Seals of Adjacent Hexagons Measured Ultrasonically vs. Photoelastically

DIMENSIONAL STABILITY

Temporal stability of the substrate material is another important parameter desirable for precision mirror blanks. After the mirror has been ground and polished, it must not change its shape due to relaxation of internal stresses or due to environmental effects. ULE has excellent long-term dimensional stability at room temperature due to negligible residual or internal strain. In a three-year study, ULE exhibited -0.14 ppm/year average length change, equivalent to -0.37 ppb/day.[8] Additional results for ULE after compressive and thermal cycling are also given in Table 2.

Table 2. Dimensional Stability Data for ULE (adapted from Justice[9])

Condition	Length change, ppm	Duration of test, days	Average length change, ppm/yr
Ambient (1st set)	-0.64	1195	-.195
Ambient (2nd set)	-0.26	1125	-.084
Uniaxial compression cycling* (0 to 14.1kg/cm^2)	-0.36	1192	-0.110
Temperature cycling* (-2° to +52°C)	+0.03	1182	+0.009

*Each cycle one hour; 1000 cycles performed within first year of testing

In a later study, the University of Arizona determined the average daily length change for ULE to be even lower, -0.17 ppb/day, with much greater precision than the earlier study.[9] In a more recent review of the subject, results by John Hall reported ULE stability to be -0.07 ppb/day (-0.025ppm/year).[10] These values are equivalent to those measured for other ultra low expansion materials, and are sufficiently low for the vast majority of applications.

Dimensional stability during thermal cycling is important when the mirror must undergo temperature cycles, for example, during application of high temperature coatings. Test data indicate that ULE exhibits no expansion hysteresis after thermal cycling.[9,11,12] That is, it returns to its original dimensions after heating or cooling, independent of the rate of temperature change. A ULE mirror exhibits no residual figure change even after the drastic change in temperature from 350°C to water quench. This is not the case for glass-ceramics which may retain permanent figure changes after thermal cycling due to structural relaxation. In some cases additional thermal treatments may reverse the effect.[13]

Another desirable parameter of a mirror material is its ability to resist distortion due to thermal gradients within the substrate. Both the thermal diffusivity and conductivity affect a mirror's performance in this area, notably so for high expansion materials. Although ULE has lower thermal conductivity and diffusivity than many other optical

materials, this is not necessarily detrimental. ULE's zero-expansivity minimizes the dimensional changes due to temperature gradients, even though it is a poor conductor. Resistance to dimensional change from thermal transients can be evaluated using a combined parameter of diffusivity k and expansivity $\alpha(k/\alpha = K/\alpha\rho C_p)$. This parameter is a better indicator of dimensional stability with thermal gradients present. Table 3 provides comparative values of this transient thermal distortion parameter. As shown in the table, the zero expansion property of ULE compensates for its relatively low conductivity and diffusivity compared to higher expansion materials. In addition, lighter weight mirror cells and active cooling can further reduce the thermal response time of a ULE mirror.

Table 3. Transient Thermal Distortion Parameter for Various Mirror Materials

Material	$k/\alpha = K/(\rho C_p \alpha)$ ($m^2 \bullet {}^\circ C/s$)
Silicon carbide	0.34
ULE™	0.27
Zerodur®	0.14
Astrositall	0.12
Beryllium	0.04

EFFECT OF RADIATION ON PROPERTIES

When used for space optics, ULE glass is exposed to high radiation which can induce electronic defects. When launched into geosynchronous orbit, low CTE materials used as mirror substrates are exposed to charged particles and gamma rays from the solar wind, solar flares, and galactic sources. In addition, when launched in circular polar orbits, they are exposed to charged particles from Van Allen belts. If the absorption coefficient is sufficiently small and/or the incident radiation is sufficiently energetic to penetrate through the depth of the sample, uniform compaction can occur. However, if the energy is deposited nonuniformly across the surface, or if it does not fully penetrate the material, the resultant compaction is nonuniform and can result in deformation, especially if the optic is thin. Higby et al[14] measured changes in the low temperature CTE value of several materials following exposure to ionizing radiation. They found significant changes in low CTE characteristics of some of these materials. Figures 3 and 4 show CTE values for ULE and Zerodur respectively before and after irradiation, over a temperature range of 125K to 325 K. It should be noted in Figure 3 that the change in ULE's CTE following irradiation is much lower than that of Zerodur at room temperature. This change is attributed to structural changes in the two-phase, fine-grained, Zerodur material and/or in the bond integrity of the crystal/glass interface. At 300 K, for example, the CTE value of ULE has increased by only 0.03 ppm/K compared with an increase of 0.23 ppm/K for Zerodur.

In another study, Rajaram et al[15] measured surface deformation of 5 to 10 mm thick slices of Optosil, ULE, Zerodur, and Astrositall following irradiation. Deformation profiles, following a radiation dose of 8.6×10^8 rads, are shown in Figure 5.

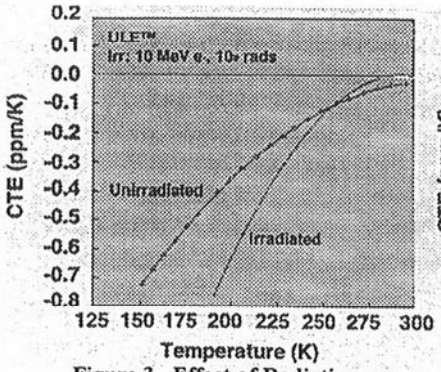

Figure 3. Effect of Radiation on CTE Values of ULE Material

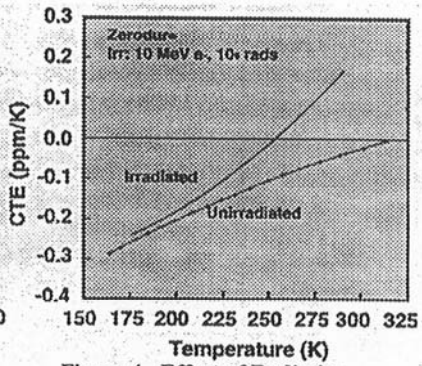

Figure 4. Effect of Radiation on CTE Values of Zerodur® Material

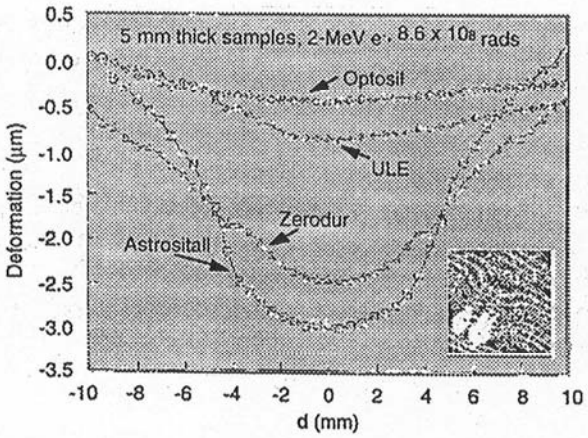

Figure 5.

Surface Deformation Profiles of Various Mirror Materials Across 20 mm Aperture Following Irradiation

The deformation pattern is nonuniform across the 20 mm diameter aperture due, primarily, to the nonuniformity of the electron beam. It is clear in this figure, however, that surface deformation is the greatest in the case of glass-ceramics. For example, for the 5 mm thick mirror, the deformation is greater than 2μm for glass-ceramics and less than 1μm for glasses. The dose dependence is shown in Figure 6. Of the four materials studied, Optosil exhibited the least amount of deformation. ULE and the two glass-ceramics follow a power law type growth with increasing dosage. However, ULE approaches saturation above 10^8 rads, whereas both Zerodur and Astrositall continue to deform above 10^8 rads.

The observed deformation is apparently related to structural rearrangement of atoms which is usually accompanied by the formation of paramagnetic defects, e.g. oxygen-associated hole centers (OHC). Good correlation was obtained between radiation-induced deformation and OHC spin concentration measured by electron spin resonance

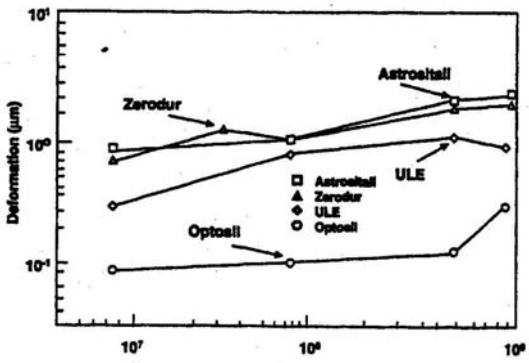

Figure 6. Effect of Radiation Dosage on Surface Deformation of Various Mirror Materials

for Optosil, Zerodur and Astrositall, indicating that OHC is the major paramagnetic defect center associated with surface deformation. Since the latter was the largest for glass-ceramics, their OHC spin concentration must be higher than that in low CTE glasses, possibly due to the presence of substantial amount of metallic constituents such as alkali and aluminum.

MECHANICAL PROPERTIES

Low density is a key property to be assessed during mirror material selection. ULE's low density compared with other common mirror materials means lighter weight optics can be made with equivalent designs. As will be shown later in this paper, however, one should try to optimize the design of a mirror for the chosen material.

The specific stiffness (defined as the ratio of Elastic modulus to density) is a measure of the mirror material's ability to resist deformation due to external forces applied during polishing, handling, mounting, launch, and operation, as well as that due to the mirror's own weight. The self-weight induced deflection of an optic is proportional to the specific stiffness, size, and shape and is not dependent on the strength of the material. ULE has nearly equivalent specific stiffness compared with other low expansion materials. Although it is lower than that of other relatively high expansion optical materials, notably silicon carbide and beryllium, a lightweight mirror design can be optimized to take advantage of ULE's zero expansion, low density, and lightweight fabrication methods, thereby minimizing mechanical differences relative to Zerodur and Astrositall. For example, although ULE has 27% lower Young's modulus than the glass-ceramics, a simple plate with 11-13% higher thickness for identical bending deformation will weigh 2.5 to 4% less than Zerodur or Astrositall. Since the ULE plate is thicker, it also will experience 22-25% lower bending stress, thereby enhancing its mechanical reliability compared to that of the glass-ceramics.[16] An indepth discussion of comparative strengths and safe design stress is given in a later section of this paper.

Another consideration in selecting a mirror material is its elastic behavior. At room temperature, ULE exhibits no measurable delayed elastic effect.[17,18] That is, after loading a 0.5cm thick polished plate of ULE with a 30 kg load over the central one inch region, while supported at three points on the edge, for two weeks, the plate resumes its

baseline optical figure within less than five minutes of unloading, compared with hours or days for glass-ceramics. This is particularly important for large lightweight optics which may undergo large strain during fabrication or due to environmental loading such as experienced in gravity release and in dynamic control of active optics.

CHEMICAL DURABILITY

Chemically, ULE has excellent resistance to weathering. It exhibits virtually no surface clouding or electrical surface leakage when subjected to attack by water, sulfur dioxide and other atmospheric gases. It also has the characteristically high resistance of silica to attack by nearly all of the chemical reagents. Rapid corrosion occurs only on exposure to hydrofluoric acid and concentrated alkaline solutions, the rate of attack increasing with temperature.

4. MIRROR FABRICATION TECHNIQUES

A brief discussion of solid mirror blanks lends insight into how Corning produces large optical blanks. The later discussion on lightweight fabrication techniques covers manufacture of all sizes of mirror blanks.

SOLID MIRRORS

Solid mirror blanks of virtually any diameter, thickness, and shape can be manufactured from ULE using Corning's fusion sealing processes. Single boules can be made into blanks up to 1.4 m diameter. Single or multiple boules can be flowed out to produce blanks from 1.4 to 2.7 m diameter. Flowout is a Corning process in which a boule or a stack of boules is heated under controlled conditions and the molten glass is flowed to the required diameter. In addition, plano discs of ULE glass can be sagged to form contoured parts. This results in lower material cost and reduced grinding time. The plano blank is placed on a refractory sag form (convex mold) and heated above the softening point allowing the glass to sag under its own weight to take the shape of the sag form; see Figure 7.

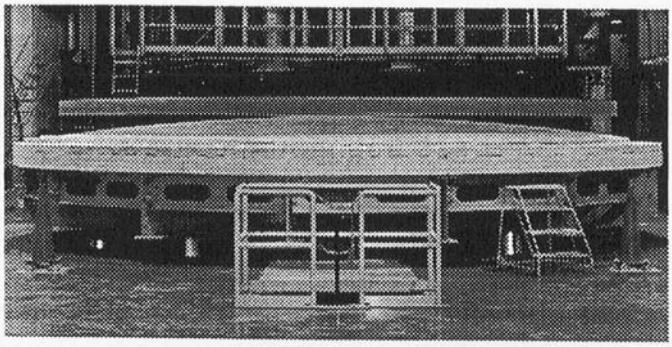

Figure 7. Sagging of 8 m Plano ULE Mirror Blank on Refractory Sag Form

For mirrors larger than 2.7 m, Corning's hex seal process can be used.[17,19] The hex seal technique uses high temperature to fusion seal hexagonal-shaped ULE or fused

silica building blocks into one monolithic piece. The hex seal process has been used successfully to produce three 8-m class meniscus mirror blanks: the 8.3 m mirror blank for the National Astronomical Observatory of Japan's SUBARU telescope and the two 8.1 m mirror blanks for the Gemini 8-M Telescopes Project. Because ULE glass can be fused with no loss in quality or strength at fusion seams, it is an ideal building block material. The hex seal process involves wire-sawing and grinding disks into hexagons, fitting together full and partial hexagons, and then fusing them at high temperature to form the mirror blank. Specifically, the manufacturing of sagged 8-m mirror blanks, depicted in Figure 8, involves the following steps:

i) fabrication of 1.5 m diameter x 15 cm thick ULE boules;
ii) stacking and fusing of two boules in a furnace to form a 30 cm thick disc;
iii) wire-sawing and grinding of above discs into hexagons of final dimensions;
iv) assemblage of full and partial hexagons in a prescribed pattern on the turntable;
v) fusing of above assembly on a rotating turntable in a furnace to form a circular blank of required diameter;
vi) grinding of the top surface using the turntable and a computer controlled grinding wheel mounted on a vertical spindle affixed to a gantry crane;
vii) turnover of the blank, using specially designed equipment, for grinding of the bottom surface;
viii) removal of the blank from the turntable for placement onto a refractory sag form for sagging in a furnace to the prescribed concave shape;
ix) controlled cooling of the sagged blank to room temperature followed by packing and shipping to the mirror polisher.

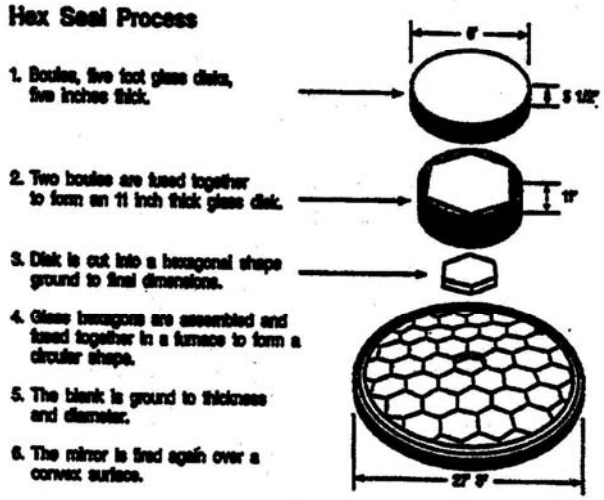

Figure 8. Corning's Hex Seal Process

Examples of mechanical reliability analyses conducted during the 8 m blank manufacture will be discussed in a later section of this paper. These large solid mirror blank fabrication processes can also be applied to the manufacture of individual components for large lightweight mirrors.

LIGHTWEIGHT MIRROR BLANKS

Fabrication techniques for lightweight mirrors range from simple machining, which removes material from the back and/or outer perimeter of a mirror blank, to various methods of bonding extremely lightweight central "cores" to front and back plates.

Machined lightweight blanks ranging from 50% to 80% lower weight can be made from ULE or fused silica using standard computer-numerical-control (CNC) machining techniques. For many applications this can result in sufficient weight reduction.

To achieve greater weight reduction, mirror blanks can be manufactured from three separate components, assembled as a "sandwich": a front plate which will be polished by conventional or advanced techniques, a central core designed to reduce mass while providing adequate support for the front plate during both polishing and mirror operation, and a back plate to provide further mechanical rigidity. The weight of the core can be as much as 97% lighter than the equivalent size solid.

Lightweight cores are typically produced using one of three methods. The first uses conventional machining, such as coredrilling circular holes or CNC machining custom-shaped holes in a solid core blank. An example of a mirror made with this technique is shown in Figure 9.

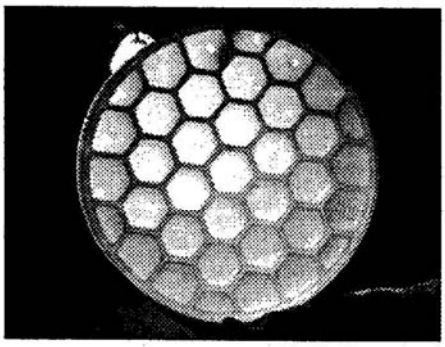

Figure 9. Lightweight ULE Mirror Blank with CNC Machined Core

The second method again takes advantage of ULE's zero expansion property, using a fusion sealing process to build lightweight core structures from building blocks. In this case, the building blocks are thin precision plates called struts which are essentially welded at ambient room temperature to produce square, rectangular, triangular, or hexagonal cell core structures. This process is shown in Figure 10, where the pre-machined struts are fused to produce cells; then the cells are fused together to produce the core structure. A more recent addition to core fabrication methods is the use of an Abrasive Water Jet (AWJ) cutting process to produce lightweight cores. Corning's AWJ machine has the largest, most powerful waterjet nozzle in the world, which has demonstrated a cutting process for 30 cm thick glass. Solids up to approximately 3 m can be lightweighted with optimized cell patterns using the machine's CNC programming capability. Cores can be optimized to accommodate special mirror mounts and can incorporate spatial nonuniform density and stiffness, if desired. Accuracy and repeatability of the AWJ system is measured in thousandths of an inch, resulting in precision core structures. Corning's first

commercial mirror blank core produced with the AWJ system is shown in Figure 11 and illustrates the flexibility of the cutting process, namely integrating thicker webs at the outer edge and central mounting hub, a hexagonal cell pattern, superimposed on an ellipse with a circular center hole.

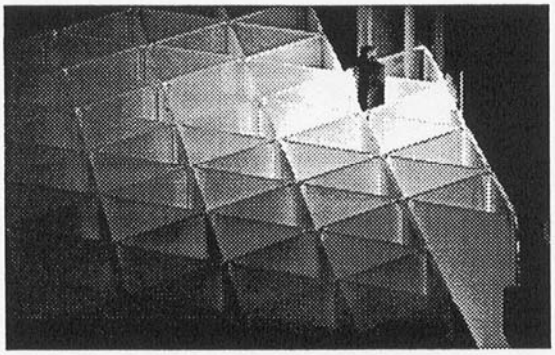

Figure 10. Fusion Sealing of ULE Core at Ambient Room Temperature

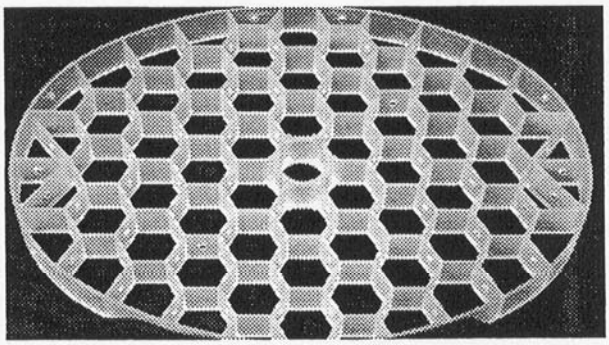

Figure 11. Intricate ULE Core Geometry Machined by AWJ Process

To take advantage of such ultra lightweight cores, two primary methods of bonding plates to the core are used. Once again, the direct fusion of glass components provides one mechanism for sealing components together. This fusion process has been used extensively for lightweight mirrors, the most notable example being the Hubble Space Telescope mirror made in the late 1970's. At the temperature required for sealing the glass together, a small amount of viscous flow must take place. This imposes minimum dimensional criteria on the mirror design in order to prevent excessive bowing and warping, thus limiting weight reduction. This limitation led Corning to develop a frit bonding process which uses a powdered glass mixed with an organic vehicle for application to the components. The thermal expansion of this frit is closely matched to that of ULE, producing strong seals with minimal residual strain. The firing of the frit takes place at temperatures below the softening point of the glass. This allows precision components to be bonded together without any deformation. The frit process thereby maintains the tight machining tolerances and allows thinner webs and plates. Table 4 compares the design characteristics of these two types of bonding.[20] Frit bonding makes core densities as low as 3% possible through the use of ultra thin components, resulting in sig-

nificant reduction in finished mirror blank weight as illustrated in Figure 12. In addition, strength testing shows that when fracture occurs, it begins in one piece of glass and crosses the frit joint into the second piece without shearing along the frit joint. The fillet geometry of the applied frit and close expansion match to ULE minimize local stress concentration at the joints. This results in higher mean seal strength.

Table 4. Design Characteristics of Fusion vs. Frit-bonded ULE Mirror

	Fusion Bonded	Frit Bonded
Minimum core density	10%	3%
Mean bond strength	2500 psi	5000 psi
Mounting blocks	Fused	Fused or fritted
Cell size	1.5-4"	1.5-6"
Minimum strut thickness	0.150"	0.050"
Average plate thickness		
Under 30" diameter	0.160"	0.100"
30 - 90" diameter	0.380"	0.300"
Over 90" diameter	0.600"	0.400"

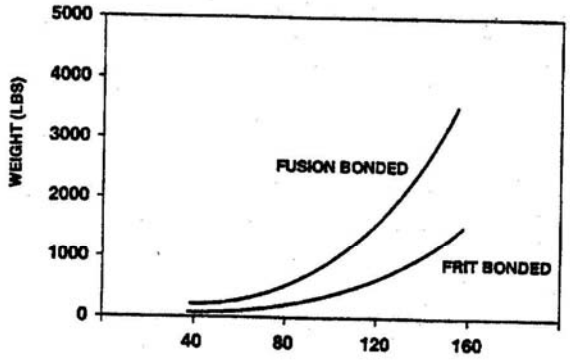

Figure 12. Comparison of Weights of Fusion vs. Frit-bonded ULE Mirrors

In short, Corning uses a wide variety of fabrication methods to achieve the required weight reduction for precision lightweight mirrors. They range from the simplest forms to advanced ultra lightweight technologies, providing the optical designer with an array of mirror blank manufacturing approaches to optimize thermal, mechanical, and optical performance.

5. MECHANICAL RELIABILITY

As noted in the preceding sections the fabrication of large monolithic ULE mirror blanks involves multiple processing steps. Each of these steps induces mechanical stresses in the mirror blank over a finite period of time. To ensure mechanical reliability of the blank, it is critical to control the stress/time history via design and process parameters thereby minimizing the growth of subsurface damage during manufacturing process[21]. Alternatively, the subsurface damage associated with grinding and polishing can be minimized via finer grit size, slower removal rate, or acid etching, all of which impose eco-

nomic penalty on the fabrication cost. However, such measures enhance the mechanical reliability of mirror blanks during fabrication, coating, transportation, installation, and operation.

The process of enhancing mechanical reliability begins with the analysis of stress/time histories the blank experiences during manufacturing and shipping. Several critical processing steps must be analyzed including rough grinding, turnover, fine grinding, acid etching, sagging, contour grinding, and packing and shipping of sagged and generated blanks. This is followed by mechanical characterization of ULE glass, involving concentric ring flexure tests on a large sample of glass discs, with different surface finishes representative of various manufacturing steps[22]. The Weibull analyses of biaxial strength and fatigue data obtained from these tests help determine the minimum strength and fatigue constant corresponding to an acceptable level of failure probability[23]. The minimum strength is further discounted to allow for large surface area of the mirror blank compared with that of disc specimens. Similarly, the Power law fatigue model helps account for finite stress duration the blank is exposed to during manufacturing by adjusting the minimum strength further[24]. In this manner, the safe stress/time history is deduced for the 8-m class blank using disc data generated in the laboratory. By safe stress we mean a stress value that will limit the failure probability of mirror blank during its manufacture to an acceptably low level, e.g. 1×10^{-6}. Verification of safe stress/time history is carried out by subjecting several groups of discs to different biaxial static stresses in 100% relative humidity for extended periods of time, representative of different manufacturing steps, and re-measuring their strength at the end of static tests. If there is no indication of strength degradation following static tests, then there is no subsurface crack growth and the recommended stress/time history for a given surface finish is indeed a safe one[21]. Conversely, the above approach helps optimize the surface finish and control subsurface damage via grinding, polishing and etching, if necessary, to sustain specified stress/time histories during the manufacture of large mirror blanks. Additional control of subsurface damage during processing also facilitates subsequent handling, packaging, and transportation of generated blanks to the polisher. A brief discussion of the factors which control the strength of silicate glasses and which help arrive at the design strength of ULE mirror blanks follows.

STRENGTH OF SILICATE GLASSES

Glass is one of the strongest materials known to mankind. This is primarily due to its non-crystalline structure with no grain boundaries and the flaw-free pristine surface. The only way glass can fracture is by cohesive failure of silicon-oxygen bonds and it takes a lot of energy to rupture these bonds. Since glass belongs to the family of brittle materials, it experiences an insignificant amount of permanent deformation prior to failure. Brittle materials are very sensitive to imperfections, defects, flaws, etc., notably those that appear on exposed surfaces [25-30]. They fail from tensile stress in the vicinity of a defect.

The above description of the nature of glass-like brittle materials can be summarized by saying that the strength of glass, to a large extent, is determined by the severity of surface flaws. Since the severity of such flaws varies from one product to another and from one user to another, the strength of glass is not a fixed property which may be found in material handbooks. Rather, it is as variable as the environment to which glass is

exposed. By environment, we mean not only the temperature, humidity, and pH level, but also the nature of loading and handling in service. Thus, unlike metals for which a definite value of strength can be quoted, glass strength must be treated more as a statistical phenomenon.

The statistical nature of glass strength forces us to either proof test on a 100% basis—an enormous undertaking—or to use a very conservative value for design strength to ensure long-term reliability. If, in addition, we allow for slow degradation of strength with stress and time—a phenomenon known as fatigue—the final design strength value will be lower yet, thus posing a challenge for efficient and cost-effective design of reliable glass products.

Theoretical estimates based on breakage of silicon-oxygen bond place the strength of pristine glass at ~2 x 10^6 psi, a value which has been verified by controlled measurements on carefully prepared specimens [31].

Yet, conventional measurements on glass specimens manufactured on a commercial scale yield a strength value of only 10,000 psi—two hundred times lower than the theoretical value! Why? Simply because glass surfaces are extremely sensitive and are easily damaged during forming, handling, assembly, packaging, shipping and daily usage.

When glass is pulled in tension, the applied stress, σ_o, appears magnified at the tip of the wedge-shaped flaw. The magnification or stress concentration factor (SCF), as developed by Griffith and refined by his followers [32,33], has the simple mathematical form involving flaw dimensions:

$$\sigma_{max}/\sigma_o = SCF = \left[1 + 2\sqrt{a/\rho}\right] \qquad (1)$$

In the above formula, a is the depth of surface flaw and ρ its tip radius; see Figure 13. Thus, for a truly sharp flaw with zero tip radius, the SCF value would approach infinity. In bulk glass the typical flaw depth and tip radius are 75 μm and 75 Å, respectively, which yield a SCF value of 200. These simple considerations explain why the strength of bulk glass is 200 times lower than the theoretical value of ~2 x 10^6 psi.

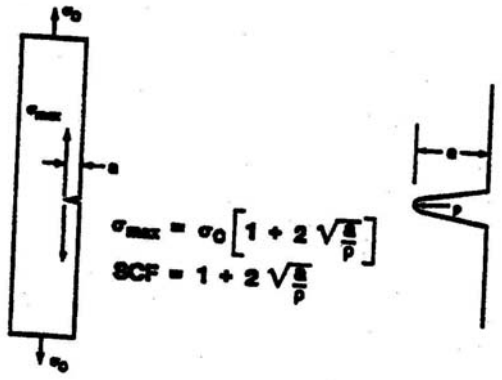

Figure 13. Stress Concentration at Griffith Flaw

There are five important experimental variables which influence the measured value of strength. They are:

a. Specimen size
b. Surface finish
c. Stress duration
d. Test environment
e. Temperature

a) With regard to size, the probability of inflicting and finding a severe surface flaw increases as the specimen size increases. Thus, the measured strength decreases as the specimen size increases.

b) Surface finish plays an important role in that it dictates the severity of surface flaws and hence the measured strength value. Table 5 is a good demonstration of the effect of surface finish on the mean strength of glass manufactured and prepared in different ways. Thus, acid etch treatment removes most of the severe flaws and yields high strength values provided the etched surface is protected immediately against further damage. Similarly, blown and drawn ware which does not come into physical contact with hard objects is stronger than pressed ware.

Table 5. Tensile Strength of Annealed Glass

Condition	Failure Stress (10^3 psi)
Fine Fibers	
Freshly drawn	500 to1000
Annealed	10 to 50
Rods, acid-etched and	
Lacquered, 1/4 inch diameter	250
Blown Ware	
Inner surfaces	15 to 40
Outer surfaces	4 to 10
Drawn window glass	8 to 20
Polished plate glass	8 to 16
Drawn tubing	6 to 15
Pressed ware	5 to 8
Ground or sandblasted surface	2 to 6

c) Glass exhibits high strength when loaded for a short period of time. During strength measurement the load is applied at a constant rate with a typical duration of about 20 to 40 seconds. If the same specimen is tested at a faster rate, as in dynamic or impact loading, one obtains significantly higher strength values (50 to 80% higher). Similarly, at slower test rates, there is a definite and appreciable decrease in measured strength. These stress rate effects are found in fibers as well as bulk glass and are due to the chemical attack of water vapor in test

environment on the stressed flaw tip, a phenomenon known as stress corrosion or fatigue [34-36]. At high loading rates the time available for fatigue is minimal, hence the strength is higher. The converse is true of low loading rates.

d) The humid environment can also have a beneficial effect on glass strength. This phenomenon, known as aging, occurs when the sharp flaw tip is rounded off by the chemical activity of water vapor in the absence of stress, thereby decreasing the stress concentration factor [29]. The extent of crack blunting and resultant strength increase depend on glass composition. In general, the higher the alkali content is, the larger the aging effect will be. Strength increases of 25-30% have been reported for aged soda-lime glass. High silica glasses like ULE do not exhibit much of an aging effect.

The above phenomena of fatigue and aging disappear when the moisture in the test environment is either absent or deactivated. Thus, the strength values obtained in vacuum or in other inert environments like liquid nitrogen are considerably higher.

The effect of electrolyte pH on glass strength has been studied by Wiederhorn [34,35]. The strength remains relatively constant for a wide range of pH values (1 to 13). Only at extreme ends of pH spectrum are strength values affected. A 10% increase is observed in the strength of soda-lime glass when tested in high pH medium. At low pH level, however, the strength is about 10% lower. The pH effect is contrary to what one might expect from stress corrosion mechanism. The current theory is that sodium for hydrogen ion-exchange takes place at the crack tip and results in strength modifications.

e) The temperature of test environment has a significant effect on measured strength. At temperatures below –50°C, water is chemically inactive and the strength is independent of temperature, loading rate and test media. Between -50°C and 250°C, the water vapor activity increases and strength decreases continually reaching a minima at 250°C. This minimum value is about 30% of inert strength value. Above 250°C, however, the strength of glasses increases, partly due to crack healing through viscous flow,exceeding the room temperature values. At still higher temperatures approaching the softening point of glass the strength begins to decrease rapidly due to viscous flow.

DESIGN STRENGTH

The design strength of annealed bulk glass is customarily taken as 1000 psi. This is the maximum value of static tensile stress which the designer of glass components may allow in service. It is based on many years of design experience, laboratory tests, customer feedback and the glass manufacturer's goal of ensuring long-term reliability. It is derived as follows:

The sandblast abrasion yields a strength value of about 6000 psi for most glasses [37,38]. However, real-life abrasion (due to excessive handling) based on strength tests on glass components which have been in service for several years tends to be twice as severe—thereby reducing

the strength to 3000 psi. Such a strength value is the amount of stress which the glass can support for short time (1 to 2 secs.). To ensure long-term reliability over a service life of 40 years or more, the short-term abraded strength must be discounted further by a factor of 3*. This reduces the strength from 3000 to 1000 psi, commonly known as the threshold value. Since crack growth at this stress level is negligibly small, glass designs based on 1000 psi service stress fall in the category of subthreshold design.

Most of the bulk glass products, as noted above, are designed and manufactured to limit the static service stress to below the threshold level. Such a subthreshold design ensures safe operation of the article throughout its lifetime and minimizes product liability cost for the glass manufacturer. In the case of telescope mirror blanks, their 8^{+}meter diameter translates into an order of magnitude larger surface area than most bulk products with higher probability of encountering critical flaws. Furthermore, their orders of magnitude greater weight poses the risk of inflicting surface damage each time they are handled during manufacturing and transportation. Finally, the acceptable failure probability for such unique, high cost, structures must be kept several orders of magnitude lower than that of most bulk glass products. These considerations reduce the design strength of ULE mirror blanks to 750 psi assuming two orders of magnitude lower failure probability than that of other bulk products.

STRESS CORROSION AND MECHANICAL RELIABILITY

The glass-ceramics, as well as ULE, contain silica as a continuous phase whose content is adjusted to achieve the ultra low thermal expansion coefficient. The Si-O-Si bond is the strongest oxide bond and renders these materials super strong, at least theoretically. However, when subjected to tensile stress in humid environment, it becomes highly reactive and transforms to Si-OH bond through a series of chemical reactions involving exchange of protons and electrons [39]; see Figure 14. The weak Si-OH bond cannot support much stress and severs easily resulting in flaw growth and gradual loss of strength. This phenomenon, known as stress corrosion cracking or static fatigue, has received much attention over the last three decades and is often used to estimate the safe allowable stress for glass structures like large telescope mirrors [21]. Since chemical reactions are activated processes, static fatigue in silicate glasses is also an activated process in which the activation energy is stress-dependent and the reaction rate is governed by both the stress field and environmental conditions at the flaw tip [40].

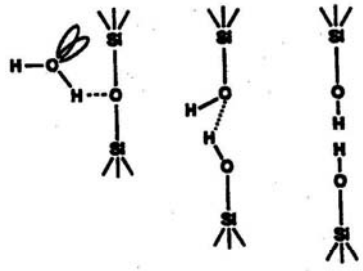

Figure 14. Stages of Stress Corrosion in Silicate Glass and Glass-ceramics

* See next section on stress corrosion and mechanical reliability.

Stress corrosion in silicate glasses is commonly described by Power law [36] which relates the rate of crack growth, da/dτ, to stress intensity, K_I, at the crack tip:

$$\frac{da}{d\tau} = AK_I^n \tag{2}$$

In eqn. 2, A and n are constants, a is crack or flaw depth, τ is time and

$$K_I = Y\sigma_a \sqrt{a} \tag{3}$$

in which Y is the flaw shape parameter and σ_a is the applied stress. The constant n is also called stress corrosion susceptibility constant, or simply fatigue constant, and is most conveniently determined by measuring the strength of glass, σ_f, as function of stress rate, $\dot{\sigma}$, in humid environment. Integration of eqn. (2) provides the following relationship:

$$\sigma_f = C(\dot{\sigma})^{1/(n+1)} \tag{4}$$

in which C is a constant. Thus, the strength of silicate glasses depends nonlinearly on the rate of stressing. Since the exponent 1/(n+1) is small for large values of n and large for small values of n, glasses with small values of n exhibit greater fatigue than those with large values of n. For example, if $n \rightarrow \infty$, the glass becomes insensitive to fatigue and its strength remains constant regardless of stressing rate.

Application of eqn. 4 to strength data at two different stress rates provides the n value

$$n = \left(\frac{\ln\dot{\sigma}_1 - \ln\dot{\sigma}_2}{\ln\sigma_1 - \ln\sigma_2}\right) - 1 \tag{5}$$

Dynamic fatigue tests for ULE glass were carried out on 15cm diameter x 6mm thick discs with 240 grit surface finish using the concentric ring fixture and 100% relative humidity (both the 240 grit grinding media and 100% RH were selected to provide a conservative value of n). Approximately 8 discs were tested at each of the four stress rates, namely 220, 22, 2 and 0.1 psi/sec. The strength vs. stress rate data are plotted on log-log scale in Figure 15. The slope of the best fit line through these data provides a measure of stress corrosion constant n per eqn. 5. A mean value of n = 41.3 is obtained from this plot with a 95% confidence interval of 24.1 to 135.1. The low end of this interval will be used for a conservative estimate of safe allowable stress during manufacturing, handling, shipping and installation of the mirror as well as in service.

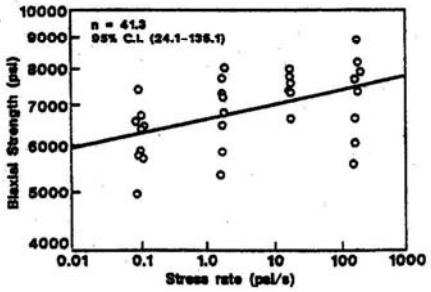

Figure 15. Dynamic Fatigue Data for ULE Discs with 240 Grit Surface in 100% RH

To assess the mechanical reliability of the mirror during the various manufacturing steps, we examine the impact of stress corrosion on design stress for each of the three mirror materials, ULE, Zerodur, and Astrositall[16]. The design stress, σ_d, is dictated by both the stressed area of mirror, A_m, relative to that of disc specimens, A_d, and the stress duration of critical manufacturing step, τ_s:

$$\sigma_d = \sigma_f \left(\frac{A_d}{A_m}\right)^{1/m} \left[\frac{(\sigma_f/\dot{\sigma})/\ (N+1)}{\tau_s}\right]^{1/n} \qquad (6)$$

In eqn. 6, σ_f denotes the specimen strength corresponding to an acceptable level of failure probability and $\dot{\sigma}$ denotes the stress rate for measuring σ_f. The most critical manufacturing step in terms of stress/time history for 8m ULE blanks is the sagging step with a duration of nearly two weeks, i.e. $\tau_s = 1.2 \times 10^6$ sec.[22]; see Figs. 16 and 17.

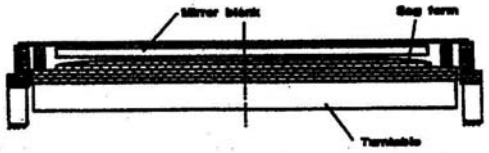

Figure 16. Schematic of ULE Mirror Blank Resting on Refractory Sagform during High Temp. Sagging

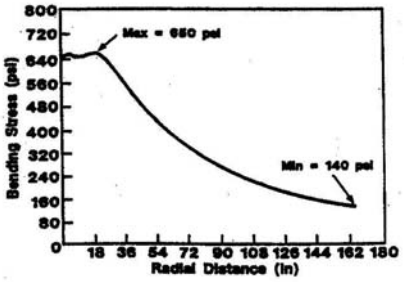

Figure 17. Bending Stress Profile on Sagform

Substituting mean MOR and stress rate values from Table 6 and using the minimum value of n from Table 7 for a conservative estimate of design stress into eqn. 6, we obtain

$$\sigma_d = 0.57\,\sigma_f (A_d/A_m)^{1/m} \tag{7}$$

for ULE and Zerodur mirrors and

$$\sigma_d = 0.53\,\sigma_f (A_d/A_m)^{1/m} \tag{8}$$

for Astrositall mirror. The effect of stressed area for identical mirror sizes should be comparable for all three materials assuming similar m values as reflected by Table 6.

Table 6. MOR Data for Mirror Candidates with 220-240 Grit Surface Finish

Mirror Material	N	MOR (psi)	Rate (psi/sec)	S.D. (psi)	m	$a_{meas.}$ (10^{-3} in)	$a_{eqn.\ 3}$ (10^{-3} in)
ULE	8	7740	220	1125	6.1	4.7	4.7
Zerodur	9	8610	180	1420	6.7	6.0	5.6
Astrositall	8	8460	180	1780	5.0	5.8	5.1

Table 7. Fracture and Fatigue Properties of Mirror Materials

Material	Fracture Toughness K_{Ic} (MPa$\sqrt{m}$)*	Stress Corrosion Constant n		
		N	Mean	95%C.I.
ULE	0.70	31	41.3	24.1-135.1
Zerodur	0.85	35	50.4	23.4-∞
Astrositall	0.80	37	34.8	20.8-98

*1 MPa$\sqrt{m}$ = 910 psi$\sqrt{in}$

For example, in the case of 8-m class ULE telescope mirror, A_d = 60 in², A_m = 6500 in², m ≈ 13 and eqns. 7 and 8 yield a design stress of 0.4 σ_f for ULE and Zerodur and 0.37 σ_f for Astrositall mirrors. Thus, it is clear that the design stress for ULE and Zerodur mirrors is an identical fraction of their failure strength and that for Astrositall mirror is slightly lower due to its lower stress corrosion constant.

For equivalent bending rigidity, the ULE mirror would be 11 to 13% thicker and would experience 22 to 25% lower stress than both Zerodur and Astrositall mirrors[16]. The lower stress offers the ULE mirror a significant advantage with respect to its long-term

reliability. According to Power law fatigue model, the predicted lifetime for ULE vs. Zerodur or Astrositall mirrors is given by[16]

$$\tau_{ULE} = \tau_{Zerodur}\left[\frac{\sigma_s^{Zerodur}}{\sigma_s^{ULE}}\right]^n \qquad (9)$$

where σ_s denotes the in-service stress which is at least 20% lower for ULE mirror. With n ranging from 20.8 for Astrositall to 24.1 for ULE, eqn. 9 predicts 100 to 200 times longer lifetime for ULE mirror than for Zerodur and Astrositall mirrors respectively. This is indeed a major advantage — one which adds confidence to mirror's lifetime mechanical reliability.

SAFE ALLOWABLE STRESS AND ITS VERIFICATION

To estimate the safe allowable stress, it is first necessary to know the stressed area A_m and stress duration τ_s of the mirror blank during its various manufacturing steps. Only two of these steps are considered critical for the ULE 8m blank due to either the high stress or long stress duration or both. These are summarized in Table 8. The safe allowable stress for the mirror blank is synonymous to design stress, namely

Table 8. Stressed Area, Maximum Stress and Stress Duration During Critical Manufacturing and Shipping Steps for ULE Mirror Blanks with Two Different Surfaces Finishes

Manufacturing Step	Stressed Area A_m (in^2)	Max. Stress Duration τ_s (sec.)	Max. Operating Stress (psi)	Surface Finish
Sagging of blank on sag form	6470	1.2×10^6	750	270/325 grit + etching
Transportation of sagged blank	960	7.9×10^6	435	120 grit

$$\sigma_d = \sigma_f\left(\frac{A_d}{A_m}\right)^{1/m}\left[\frac{(\sigma_f/\dot{\sigma})/(n+1)}{\tau_s}\right]^{1/n} \qquad (10)$$

Tables 9 and 10 provide the total disc area subjected to stress σ_d, corresponding to a failure probability of 1×10^{-6}, for an equivalent static duration of $[(\sigma_d/\dot{\sigma}) / (n + 1)]$, together with the pertinent Weibull slopes and fatigue constants representing the surface finish relevant to the two critical manufacturing steps. The 270/325 grit finish followed by acid etching was deemed appropriate for the sagging step due to high stress and relatively long stress duration. Similarly, the 120 grit finish was selected for those areas of mirror

blank subjected to lower stress over an extended period of time during its transportation to the polisher.

Table 9. Strength of ULE Discs Corresponding to Failure Probability of $1x10^{-4}$

Surface Finish	σ_d ($P_f = 1x10^{-4}$) (psi)	No. of Discs Tested	Total Area Ad Subjected to Max. Stress σ_d (in^2)
120 grit	3430	20	54
120 grit + etching	3050	19	51
270/325 grit	4720	25	67
270/325 grit + etching	3175	22	59

Table 10. Stressed Area, Stress Duration, Weibull Slope and Fatigue Constant for ULE Discs with Two Different Surface Finishes

Manufacturing Step	Max. Disc Area A_d (psi)	Equivalent Static Duration for Strength Measurement (sec.)	Weibull Slope m	Fatigue Constant n	Surface Finish
Sagging of blank on sag form	59	1.65	13.2	24.1	270/325 grit + etching
Transportation of sagged blank	54	1.20	24	24.1	120 grit

Using the data in Tables 8, 9 and 10, both the area reduction factor and fatigue factor in eqn. 6 can be computed. The safe allowable stress σ_s is then estimated by using eqn.10 and σ_d values from Table 9.

Table 11. Estimate of Safe Allowable Stress for ULE Mirror Blank during its Critical Manufacturing and Shipping Steps for Failure Probability of $1x10^{-4}$

Manufacturing Step	Disc Strength at $P_f = 1x10^{-4}$ (psi)	Area Reduction Factor	Fatigue Factor	Safe Allowable Stress σ_s (psi)	Max. Operating Stress (psi)
Sagging of blank on sag form	3175	0.70	0.65	1450	750
Transportation of sagged blank	3430	0.89	0.60	1820	435

The results of these computations are summarized in Table 11 which also shows the maximum operating stress on mirror blank during sagging and shipping. Let us note that the allowable stress is nearly 2 to 4 times larger than the operating stress providing an additional safety margin for high reliability during manufacturing. These safety margins are direct consequence of high m and n values, i.e. low variability in strength distribution due to consistent finishing process and high fatigue resistance of ULE glass.

To verify the ultimate reliability of a mirror blank eight discs with 270/325 grit surface finish plus acid etching were subjected to a static biaxial stress of 800 psi in 100% RH for 14 days. Their strengths were re-measured after 14 days and found to be identical to the initial distribution as shown in Figure 18. This confirmed that the sag form stress of 750 psi was below the threshold value for acid-etched 270/325 grit surface finish and would not lead to slow crack growth. Needless to say, all of the 8-m class mirror blanks manufactured at Corning to date have survived the sagging stresses with no evidence of flaw growth. Similarly, to evaluate the reliability of a generated mirror blank, ten ULE discs with 120 grit surface finish were subjected to a static biaxial stress of 435 psi in 100% RH for 90 days. Their strength was re-measured after 90 days and found to be identical to the initial distribution as shown in Figure 19.

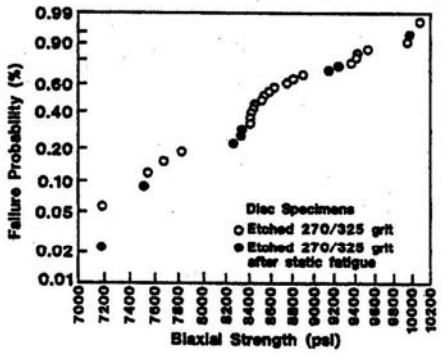

Figure 18. Effect of Static Stress on Strength Distribution of ULE Discs with 270/325 Grit Surface: σ_s = 800 psi, τ = 14 days, T = 25°C, RH = 100%

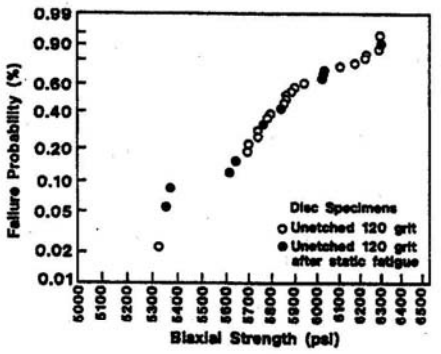

Figure 19. Effect of Static Stress on Strength Distribution of ULE Discs with 120 Grit Surface: σ_s = 435 psi, τ = 90 days, T = 25°C, RH = 100%

Thus, no slow crack growth is expected on the 120 grit surface due to a long-term static stress of 435 psi. It is worth pointing out that the additional safety factor of two to four in the above computations not only promotes mechanical reliability of mirror blanks, it does so at an ultra low failure probability $< 1 \times 10^{-6}$ as may be verified from Weibull distribution function given by eqn. (11)[22].

$$P_f = 1\text{-}\exp\left[-(\sigma/\sigma_o)^m\right] \qquad (11)$$

Thus, the mechanical reliability of very large monolithic mirror blanks during their fabrication requires thorough understanding of stress/time history at each of the manufacturing steps. Such knowledge helps select an appropriate surface finish with strength and fatigue characteristics capable of sustaining manufacturing stresses without measurable crack growth in corrosive environment. The latter is ascertained by comparing strength distributions before and after subjecting a large sample of glass discs to static stress in corrosive environment over a finite period of time, representative of the process, and making sure that the two distributions are indistinguishable. Thus, a 270/325 grit surface finish is deemed appropriate for the sagging step which induces a static stress of 650 psi over the two-week period, and a 120 grit surface finish is appropriate for transporting the mirror blank which induces a static stress of 435 psi over the three-month period.

The use of biaxial strength and fatigue data, obtained by testing a large sample of 15 cm discs, together with Weibull distribution helps estimate a safe allowable stress for the mirror blank during its manufacture and transportation taking full account of stress/time history, test environment and ultra low failure probability.

The analysis of deflection and stresses shows that optimum mirror design, using low expansion materials like ULE, Zerodur and Astrositall, can be achieved by maximizing the specific bending rigidity while minimizing both manufacturing and operating stresses for ensuring long-term mechanical reliability[16]. Indeed, such an analysis helps compute the mirror thickness for equivalent bending rigidity of the three materials. In view of its 27% lower Young's modulus, the ULE mirror must be 11 to 13% thicker than Zerodur and Astrositall mirrors of identical diameter. The higher thickness, however, does not pose a weight penalty in view of 13% lower density of ULE glass relative to that of Zerodur and Astrositall. On the contrary, it helps reduce bending stress in the ULE mirror by up to 25% thereby promoting its long-term mechanical durability by 100 to 200 times compared with Zerodur and Astrositall mirrors[16].

6. ADVANCES IN ULE™ GLASS

Anyone who has not utilized ULE in several years will note marked improvement in the quality of the material itself. Corning has also improved CTE measurement precision giving engineers more accurate expansion data with which to design mirror blanks. There are fewer and smaller inclusions in the glass when compared to that which was produced years ago. CTE homogeneity within the boule and between boules is practically negligible as shown by the success of the Corning 8 meter mirror blanks.

Process improvements continue in the material and mirror manufacturing

processes. The world's most powerful abrasive water jet machine enables optical designers more freedom to design mechanically stiff and more lightweight mirrors for advanced applications. Corning has effected changes in technology in the more traditional strut-fusion core manufacturing processes yielding lightweight cores with higher strength. Ongoing improvements include new developments of glass fusion processes.

Corning is currently working on new glass forming processes utilizing different raw materials and technological advances that will foster the tradition of continuous improvement.

7. SUMMARY

ULE, titania-silica binary glass, offers an optimum combination of mechanical, thermal and optical properties which make it an ideal material for precision optical structures and lightweight telescope mirrors. Its near-zero expansion, controlled by titiania content over the operating temperature range helps preserve the figure; the absence of hysteresis in its thermal expansion curve ensures dimensional stability of the mirror in extreme environments; its low density affords high specific stiffness thereby reducing the elastic deformation of lightweight structures; its high fatigue resistance permits higher long-term stress, hence lightweight mirror structure, without compromising long-term mechanical integrity; and its excellent optical and birefringence properties facilitate inspection and quality assurance in terms of index homogeneity, defect level and residual strain.

Following a review of critical material requirements and key physical properties, the paper discusses the fabrication techniques for both solid and lightweight mirror blanks. It shows that a wide variety of fabrication methods is available for achieving the required weight reduction for precision lightweight mirrors. They range from the simplest forms to advanced ultra lightweight technologies, providing the optical designer with an array of mirror blank manufacturing approaches to optimize thermal, mechanical, and optical performance. The mechanical reliability of very large monolithic mirror blanks during their fabrication requires thorough understanding of stress/time history at each of the manufacturing steps. Such knowledge helps select an appropriate surface finish with strength and fatigue characteristics capable of sustaining manufacturing stresses without measurable crack growth in corrosive environment. The latter is ascertained by comparing strength distributions before and after subjecting a large sample of glass discs to static stress in corrosive environment over a finite period of time, representative of manufacturing process, and making sure that the two distributions are indistinguishable.

The analysis of deflection and stresses shows that optimum mirror design, using low expansion materials like ULE, Zerodur, and Astrositall, can be achieved by maximizing the specific bending rigidity while minimizing both manufacturing and operating stresses. Indeed, such an analysis helps compute the mirror thickness for equivalent bending rigidity of the three materials. In view of its 27% lower Young's modulus, the ULE mirror must be 11 to 13% thicker than Zerodur and Astrositall mirrors of identical diameter. The higher thickness, however, does not pose a weight penalty in view of 13% lower density of ULE glass than that of Zerodur and Astrositall. On the contrary, it helps reduce bending stresses in the ULE mirror by up to 25% thereby promoting its long-term mechanical durability by 100 to 200 times compared with Zerodur and Astrositall mir-

rors.

The paper concludes with a brief review of advances in fabrication of ULE mirrors. These include different raw materials and alternate forming processes which allow higher production volumes without compromising glass quality and physical properties. Finally, improvements in CTE measurement precision should give engineers more accurate expansion data with which to design mirror blanks. There are also fewer and smaller inclusions in the boules compared with those made years ago, and the homogeneity of CTE within a boule and between boules is excellent, as shown by the success of Corning 8-meter ULE mirror blanks.

8. ACKNOWLEDGEMENT

The authors are grateful to Virginia Doud, Nancy Gleason and Nancy Foster of the Science and Technology Division for their able assistance in the completion of this paper. Valuable discussions with Joe Neubert, Tom Hobbs, Don Kloeber, Richard Smith and Bob Jones of the Lighting and Materials Division are greatly appreciated.

9. REFERENCES

[1]Yoder, Paul R., "Opto-Mechanical Systems Design," Optical Engineering, Vol. 9, Marcel Dekker, Inc., New York, 1986, p.72.

[2]Barnes Jr., William P., "Optical Materials - Reflective," Applied Optics and Optical Engineering, Vol. 7, Academic Press, Inc., 1979, Chapter 4, pp. 97-119.

[3]Cho, M. K., and Powell, William R., "Thermal analysis on hexagonal placement patterns of the Gemini primary mirrors," Proceedings of SPIE, Vol. 2857, August 1996.

[4]Sasaki, A., Mikami, I., Shimoyama, N., Nishiguchi, K., Powell, W.R., Edwards, M.J., Ando, H., and Iye, M., "Primary mirror blank fabrication of Subaru Telescope," Proceedings of SPIE, Vol. 2199, pp. 156-161, March 1994.

[5]Hagy, H.E., ""A Review of Measurement Systems for Evaluating Thermal Expansion Homogeneity of Corning Code 7971 ULE™," Proceedings of SPIE, Vol. 1533, pp. 198-209, July 1991.

[6]Edwards, M.J., Bullock, E.H., and Morton, D.E., "Improved precision of absolute thermal expansion measurements for ULE™ glass," Proceedings of SPIE, Vol. 2857, pp. 58-63, August 1996.

[7]Hagy, Henry E. and Best, Michael E., "Comparison of two high-precision nondestructive measurement methods for evaluating thermal expansion differences in the 8.3-m ultralow-expansion Subaru primary mirror blank," Applied Optics, Vol. 35, No. 7, pp. 1126-1128, 1 March 1996.

[8]Justice, B., "Precision Measurements of the Dimensional Stability of Four Mirror Materials," Journal of Research of the National Bureau of Standards, Vol. 79A, No. 4, pp. 545-550, 1975.

[9]Berthold III, J.W.. Jacobs, S.F., and Norton, M.A., "Dimensional stability of fused silica, Invar, and several ultralow thermal expansion materials," Applied Optics, Vol. 15, No. 8, pp.1898-1899, August 1976.

[10]Jacobs, S.F., "Variable invariables - dimensional instability with time and temperature," Proceedings of SPIE, Vol. CR43, pp. 181-204, July 1992.

[11]Jacobs, S., "Effect of Thermal Cycling," final report, Air Force Weapons Laboratory, AFWL-TR-87-20, May 1988.

[12]Jacobs, S., et al, "Surface figure changes due to thermal cycling hysteresis," Applied Optics, Vol. 26, No. 20, 15 October 1987.

[13]Lindig, Otto, and Pannhorst, Wolfgang, "Thermal expansion and length stability of Zerodur in dependence on temperature and time," Applied Optics, Vol. 24, No. 20, pp. 3330-3334, 15 October 1985.

[14]Higby, P.L., Askins, C.G., Ruller, J.A., and Friebele, E.J., "Radiation effects on the low temperature coefficient of thermal expansion of low-CTE materials," Proceedings of SPIE, Vol. 970, pp. 70-77, 1988.

[15]Rajaram, M., Tsai, T., and Friebele, E.J., "Radiation-induced Surface Deformation in Low-Thermal-Expansion Glasses and Glass-Ceramics," Advanced Ceramic Materials, Vol. 3, Number 6, pp. 598-600, 1988.

[16]Gulati, S.T., "Design considerations for mirror materials," Proceedings of SPIE, Vol. 2857, pp. 2-11, August 1996.

[17]Pepi, John W. and Golini, Donald, "Delayed elastic effects in the glass ceramics Zerodur and ULE at room temperature," Applied Optics, Vol. 30, No. 22, pp. 3087-3088, 1 August 1991.

[18]Pepi, John W. and Golini, Donald, "Delayed elasticity in Zerodur at room temperature," Proceedings of SPIE, Vol. 1533, pp. 212-221, July 1991.

[19] Smith, R. K., Edwards, M. J., Kloeber, D. B., "Fabrication of Subaru primary mirror blank," Proceedings of SPIE, Vol. 2199, pp. 901-910, March 1994.

[20]Spangenberg-Jolley, J. and Hobbs, T., "Mirror substrate fabrication techniques of low expansion glasses", Proceedings of SPIE, Vol. 966, pp. 284-290, 1988.

[21]Gulati, S.T.; "Dynamic and Static Fatigue of Silicate Glasses under Biaxial Loading: Application to Space Windows, CRTs and Telescope Mirrors," 5th International Otto

Schott Colloqium, Jena Germany; July 10-14, 1994.

[22]Gulati, S.T. and Powell, W.R., "Mechanical Reliability of 8m Class ULE'Glass Telescope Blanks during Manufacturing, "SPIE Proc.; 2546 (1995).

[23]Weibull, W.; "A Statistical Distribution Function of Wide Applicability; "J. App. Mech., Vol. 18; 1951.

[24]Gulati, S.T., "Optimization of Surface Finish of 8m Class ULE'Glass Telescope Mirror Blanks for Lifetime Mechanical Reliability, "SPIE Proc., 2774 (1996).

[25]Ernsberger, F.M.; "Strength of Glasses,"Proc. 8th Int'l Cong. on Glass, London; 1968.

[26]Phillips, C.J.; "The Strength and Weakness of Brittle Materials," American Scientist; 1965.

[27]Field, J.E.; "Brittle Fracture: its Study and Application," Contemp. Phys.; 1965.

[28]McLellan, G.W. and Shand, E.B.; Glass Engineering Handbook, 3rd Ed.; McGraw-Hill, New York, 1984.

[29]Mould, R.E.; "Strength and Static Fatigue of Abraded Glasses Under Controlled Ambient Conditions: Parts, I, II, III & IV; "J. Am. Ceram. Soc., Vol. 44, No. 10; 1961.

[30]Kerper, M.J.; Lathey, C. and Robinson, E.R.; "Properties of Glasses at Elevated Temperatures, "WADC Tech. Report-56-645, Part I, National Bureau of Standards, Washington, D.C.; 1956.

[31]Kurkjian, C.R. and Paek, U.C.; "Single-Valued Strength of Perfect Silica Fibers; "Appl. Phys. Letter, Vol. 42, No. 3; 1983.

[32]Griffith, A.A.; "The Phenomena of Rupture and Flow in Solids, "Phil. Trans. Roy. Soc., Vol. A221; London; 1920.

[33]Ingis, C.E.; "Stresses in a Plate due to Presence of Cracks and Sharp Corners," Trans. Inst. Nav. Archit., Vol. 55; 1913.

[34]Wiederhorn, S.M. and Bolz, L.H.; "Stress Corrosion and Static Fatigue of Silicate Glass," J. Am. Ceram. Soc., 53, 10 (1970).

[35]Wiederhorn, S.M.; "Subcritical Crack Growth in Ceramics, "Fracture Mech. of Ceramics, Plenum Press, New York; 1974.

[36]Ritter, J.E. and Sherburne, C.L.; "Dynamic and Static Fatigue of Silicate Glasses;" J.Am. Ceram. Soc., 54, 12 (1971).

[37]Kerper, M.J.; Lathey, C. and Robinson, E.R.; "Properties of Glasses at Elevated Temperatures," WADC Tech. Report-56-645, Part I, National Bureau of Standards,

Washington, D. C.; 1956.

[38]Kerper, M.J. and Scuderi, T.G.; "Modulus of Rupture in Relation to Fracture Pattern;" Ceramic Bulletin, Vol. 43, No. 9; 1964.

[39]Mecholsky, J.J.; Freiman, S.W. and Morey, S.M.; "Fractographic Analysis of Optical Fibers," Ceramic Bulletin, Vol. 56, No.11; pp. 1016-1077; 1977.

[40]Gulati, S.T. and Glaesemann, G.S.; "Design Methodology for the Mechanical Reliability of Optical Fiber;" Optical Engineering Journal; 1991.